Probing the strong electroweak symmetry breaking in a model with a vector resonance

M. Gintner[1,2], I. Melo[1], B. Trpišová[1]

[1] *Physics Department, University of Žilina, Žilina*
[2] *Science and Research Institute, Matej Bel University, Banská Bystrica*

Abstract

We systematically study the possibility to probe the physics behind the electroweak symmetry breaking at the LHC assuming new strong interactions being responsible for the effect. The new physics is described by the Higgs-less effective Lagrangian with a vector resonance in the particle spectrum, in addition to the Standard Model fields. We analyze signals of the resonance in the mixing-induced LHC processes $pp \to abX$, $ab = t\bar{t}, b\bar{b}, t\bar{b}, W^+Z, W^+W^-$. At this level of our calculations we do not consider further decays of the quarks and of the gauge bosons.

Introduction

Despite the great success of the Standard model of electroweak interactions (SM) one essential component of the theory remains a puzzle: it is the actual mechanism behind the electroweak symmetry breaking (ESB). The Higgs complex doublet scalar field of a non-zero vacuum expectation value serves as a benchmark hypothesis for the mechanism. It is not the only plausible hypothesis though. A direct consequence of the Higgs hypothesis is the presence of the Higgs boson in the particle spectrum of the SM, not observed to these days.

There is a host of candidates for the suitable extensions of the SM. They range from supersymmetric theories with multiple elementary Higgs bosons in their spectra to the theories of new strong interactions, like in Technicolor, which might form bound states of new elementary particles in analogy with QCD. These bound states might appear in the particle spectrum as new resonances.

In more recent theories like the Little Higgs models and the Gauge-Higgs unification models, their dual-description relation to the Heavy Composite Higgs and the No Higgs strongly-interacting models has been demonstrated (see [1] and references therein). Most of these new models introduce new quarks and new vector particles at about 1 TeV.

Facing this plethora of alternative theories it is highly desirable to describe their low-energy phenomenology in a unified way. Thus, it is very useful to exploit the formalism of effective Lagrangians. We use the so-called *hidden local symmetry* (HLS) approach [2] to introduce the new vector resonance. The HLS formalism along with the AdS/CFT correspondence plus deconstruction is also behind the dual-description relation of the recent models mentioned above [1].

In our model, the new $SU(2)_V$ vector bosons mix with the electroweak gauge bosons. While the mixing complicates theoretical analysis of the model it might provide some advantages in experimental searches. It is natural to assume that apart from the electroweak gauge bosons the new vector triplet couples to the third generation of quarks only. Therefore it would seem natural to search for the signs of the new resonances in the processes where besides the electroweak bosons the t and b quarks are involved. At the LHC this is often a difficult case due to the large backgrounds to the processes with b and t in the final state and/or due to the negligible b and t luminosities in pp collisions. However, the mixing of the vector resonances with the electroweak gauge bosons generates interactions of the new resonances to the fermions of lighter generations. Although these interactions are suppressed by the mixing factors, the processes enabled by them have the advantage of higher parton luminosities and more favorable final state topologies, on the other hand.

In the next section we briefly introduce our effective Lagrangian. In the following section we present results of our analysis. In Conclusions we summarize our findings and outline the prospective steps of this investigation.

Lagrangian

Our Lagrangian is based on the non-linear Callan-Coleman-Wess-Zumino Lagrangian [3, 4]. This approach was applied in formulating the so-called BESS (Breaking Electroweak Symmetry Strongly) model (e.g. [5] and references therein) which pioneered the use of the HLS approach to the effective description of new resonances formed by new strong interactions related to the ESB.

The BESS model considered in the literature possesses the ρ-to-fermion coupling inter-generation universality [5] which leads to stringent limits on these couplings from the existing measurements of the SM parameters. In an attempt to reflect the speculations about a special role of the top quark (or the third quark generation) in the mechanism of ESB we modify the fermion sector by considering no direct interactions of ρ to the fermions other than t and b. In addition, the $SU(2)_L$ symmetry does not allow us to disentangle the ρ-to-t_L coupling from the ρ-to-b_L one. However, it can be done in the case of right fermions. We do it and to simplify the numerical analysis of the model we turn off completely the direct interaction of ρ to b_R. The full form of our Lagrangian can be found in [6]. Here, we show only the part responsible for interactions of t and b quarks to the new vector resonances as well as non-SM interactions of t and b to the SM gauge bosons

$$L_\rho^{(t,b)_L} = \frac{b_1}{1+b_1} g\, \bar{\psi}_L \not{W}_a \tau_a \psi_L + \frac{b_1}{1+b_1} g_V\, \bar{\psi}_L \not{\rho}_a \tau_a \psi_L \qquad (1)$$

$$L_\rho^{(t,b)_R} = \frac{b_2}{1+b_2} g' (\bar{\psi}_R P_0)\, \not{B} \tau_3 (P_0 \psi_R) + \frac{b_2}{1+b_2} g_V (\bar{\psi}_R P_0)\, \not{\rho}_3 \tau_3 (P_0 \psi_R) \qquad (2)$$

where $\psi = (t,b)^T$, and $P_0 = \mathrm{diag}(1,0)$. As a consequence of turning off the ρ-to-b_R coupling neither t_R directly couples to the charged ρ-resonance, as can be seen in (2).

The measurement of $Zb\bar{b}$ vertex constrains the ρ-to-t_L coupling to relatively small values. However, when the disentangling is applied the measurement does not limit the ρ-to-t_R interaction. For the low-energy limits on the model parameters, see [7].

Two-particle final state processes: analysis and results

We test the model when the mass of the neutral ρ-resonance is $M_{\rho^0} = 1$ TeV. Depending on the model parameters ρ^0 decays predominantly through one or more of the following three channels: $t\bar{t}$, $b\bar{b}$, W^+W^-. When its mass is fixed the total width of ρ^0, as well as its branching ratios, depend on g_V, b_1, and b_2. The situation in the $g_V - b_1 - b_2$ parametric space is depicted in Figure 1. Note that due to the turning off of the ρ-to-b_R coupling there is no such a choice of parameters when the decay of ρ^0 either solely to $b\bar{b}$ or to both, $b\bar{b}$ and W^+W^-, dominates.

The parameters M_{ρ^0}, g_V, b_1, and b_2 also determine the mass of $\rho^\pm$ and its decay width and branching ratios. The $\rho^\pm$-resonance dominantly decays to $t\bar{b}/\bar{t}b$ and/or $W^\pm Z$. In Table 1 we show the points of the $g_V - b_1 - b_2$ parametric space we test in our calculations.

We begin with the analysis of two-particle processes not only because they are the simplest ones to calculate but also to demonstrate that the visible ρ-resonance peaks can appear even in the presence of the mixing-suppressed couplings. We implemented our Lagrangian [6] into the CompHEP software [8, 9] as one of its models. Numerical analysis was performed at the selected points of the parametric space. All calculations have been performed at tree level.

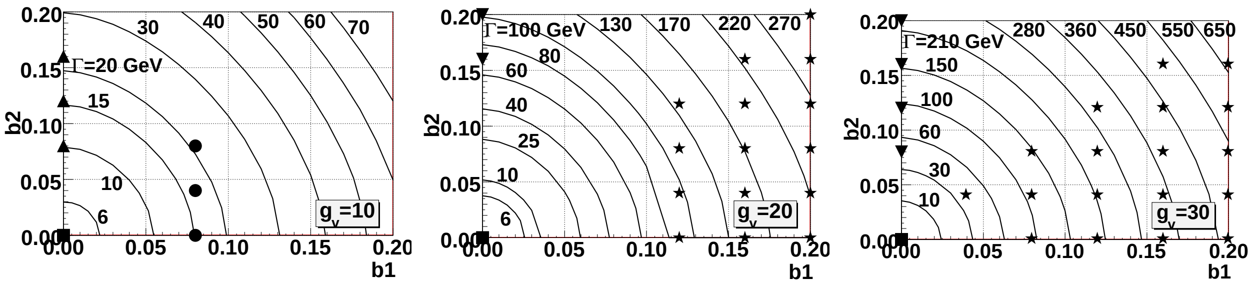

Figure 1: The total widths of ρ^0 depicted in the $g_V - b_1 - b_2$ parametric space. The markers distinguish areas of a clear domination of some channels; circles: $t\bar{t} \sim b\bar{b} \sim W^+W^-$, squares: $W^+W^- \gg t\bar{t}, b\bar{b}$, down-pointing triangles: $t\bar{t} \gg b\bar{b}, W^+W^-$, stars: $t\bar{t}, b\bar{b} \gg W^+W^-$, up-pointing triangles: $t\bar{t}, W^+W^- \gg b\bar{b}$.

P	g_V	b_1	b_2	Γ_{ρ^0} (GeV)	BR(ρ^0) W^+W^-	BR(ρ^0) $t\bar{t}$	BR(ρ^0) $b\bar{b}$	$M_{\rho^\pm}$ (GeV)	$\Gamma_{\rho^\pm}$ (GeV)	BR($\rho^\pm$) $t\bar{b}/\bar{t}b$	BR($\rho^\pm$) $W^\pm Z$
1	10	0.08	0.04	16.899	31%	38%	31%	999.84	15.281	64%	36%
2	10	0.12	0.04	28.256	19%	42%	39%	999.84	26.433	79%	21%
3	10	0	0	5.334	99%	0.12%	0.08%	999.84	5.443	0.2%	98%
4	20	0	0.12	42.788	3%	97%	0.0025%	999.96	1.358	0.2%	98%
5	20	0.08	0	42.471	3%	46%	51%	999.96	42.509	97%	3%
6	35	0.04	0	34.580	1%	47%	52%	999.99	34.594	99%	1%
7	10	0	0.08	10.169	52%	48%	0.042%	999.84	5.443	0.18%	98%

Table 1: Properties of the ρ-triplet in the selected points of the $g_V - b_1 - b_2$ parametric space when $M_{\rho^0} = 1$ TeV.

There have been five two-particle processes analyzed. They are listed in Table 2. The cuts have been introduced to maintain numerical stability of the calculations or to simulate the blind angle of the detector. No attempt to improve the signal-to-background ratio using cuts has been made.

We would like to know if the LHC signal by our model can be distinguished from the LHC signal of the SM with the Higgs boson of the mass $M_{Higgs} = 115$ GeV. For that purpose we calculate the statistical significance of the model signal with respect to the SM

$$R = \frac{N_P - N_{SM}}{\sqrt{N_{SM}}}$$

where N_P and N_{SM} are the numbers of the events of our model and the SM, respectively. It is customary to consider as statistically significant such a deviation for which $R > 5$. We calculate R's based on the total cross sections as well as on the cross sections in the vicinity of the ρ peak, $0.7\ \text{TeV} \leq m_{34} \leq 1.1$ TeV, where m_{34} is the final state pair of particles invariant mass. No reducible backgrounds and no improving cuts are considered at this stage. Since $pp \to t\bar{t}X$ and $pp \to b\bar{b}X$ are plagued by gluon-gluon backgrounds we focus on the remaining three processes in our calculations. The obtained results are shown in Table 3.

Since none of the final state particles of the studied processes is stable, it is more relevant to consider the statistical significance when the decays are taken into account. In addition, also the question of detection efficiency of a given final state is important in evaluating more realistic values of R. In our calculations we consider the following reduction factors for the observed number of events: the efficiency of the b-jet detecting $\epsilon_b = 0.5$; the branching ratio $b^W_{jj} = \text{BR}(W \to jj) = 0.64$, where j is a light-quark jet; $b^W_{\ell\nu} = \text{BR}(W \to \ell\nu_\ell) = 0.11$, where ℓ is one of the charged SM leptons; $b^Z_{\ell\ell} = \text{BR}(Z \to \ell^-\ell^+) = 0.034$; $b^Z_{jj} = \text{BR}(Z \to jj) = 0.538$; $b^Z_{bb} = \text{BR}(Z \to b\bar{b}) = 0.153$. The obtained

process	subprocess	P	ρ-peak visible	σ (pb)	cuts
$pp \to t\bar{t}X$	$gg \to t\bar{t}$	1–7	no	726	no
	$b\bar{b} \to t\bar{t}$	6	yes	1.69	
$pp \to b\bar{b}X$	$gg \to b\bar{b}$	1–7	no	1120	$m_{b\bar{b}} \geq 350$ GeV
	$b\bar{b} \to b\bar{b}$	5	yes	22.5	$-0.95 \leq c_{13}, c_{14} \leq 0.95$
$pp \to t\bar{b}X$	$u\bar{d} \to t\bar{b}$	2	yes	1.96	$-0.99 \leq c_{13}, c_{14} \leq 0.99$
	$c\bar{s} \to t\bar{b}$		yes	0.29	
	$u\bar{d} \to t\bar{b}$	5	yes	1.99	
	$c\bar{s} \to t\bar{b}$		yes	0.30	
	$u\bar{d} \to t\bar{b}$	SM	N/A	1.85	
	$c\bar{s} \to t\bar{b}$		N/A	0.28	
$pp \to W^+W^-X$	$u\bar{u} \to W^+W^-$	2	no	14.02	$-0.99 \leq c_{13}, c_{14} \leq 0.99$
	$b\bar{b} \to W^+W^-$		yes	0.77	
	$u\bar{u} \to W^+W^-$	3	yes	14.02	
	$b\bar{b} \to W^+W^-$		yes	0.74	
	$u\bar{u} \to W^+W^-$	SM	N/A	13.13	
	$b\bar{b} \to W^+W^-$		N/A	0.70	
$pp \to W^+ZX$	$u\bar{d} \to W^+Z$	1	yes	5.27	$-0.99 \leq c_{13}, c_{14} \leq 0.99$
	$c\bar{s} \to W^+Z$		yes	0.91	
	$u\bar{d} \to W^+Z$	3	yes	5.28	
	$c\bar{s} \to W^+Z$		yes	0.91	
	$u\bar{d} \to W^+Z^-$	SM	N/A	4.60	
	$c\bar{s} \to W^+Z^-$		N/A	0.79	

Table 2: Properties of the analyzed two-particle final state processes at $\sqrt{s} = 14$ TeV. Only the most important and interesting subprocesses and points P of the parametric space are displayed. The cross section values correspond to the $q\bar{q}' + \bar{q}'q$ initial states of the subprocesses. The SM results are calculated assuming $M_{Higgs} = 115$ GeV; c_{13} and c_{14} denote cosines of the scattering angles of the first and the second final state particles, respectively.

statistical significance for the processes after the final state decay is shown in Table 4.

We can see that the highest yields and statistical significance is in the channels that involve hadrons. At the same time though, these will be the channels with the richest and the most complicated backgrounds to deal with. The leptonic channels exhibit lesser event yield and lesser sensitivity. On the other hand, they provide cleaner signal and easily detectable particles, like muons. Thus, when selecting the most appropriate channels for probing our model it has to be a tradeoff between advantages and disadvantages of the both worlds. In addition, many of the channels displayed in Table 4 can be combined to reach higher statistics and/or complementary information on the properties of the model.

Conclusions

With the start of the LHC new era in attacking the question of the ESB mechanism begins. In this paper we have investigated the potential of the LHC processes $pp \to abX$, $ab = t\bar{t}, b\bar{b}, t\bar{b}, W^+Z, W^+W^-$, to probe a new vector $SU(2)_V$ triplet which might exist as a part of new physics responsible for ESB and, as far as fermions are concerned, it interacts directly to the third quark generation only. It is possible that new physics behind ESB can be effectively described by the HLS approach. Then the mixing of the vector resonances with the electroweak gauge bosons induces also interactions of ρ to

process	P	cut	σ (pb)	R_0	R (100 fb^{-1})
$pp \to t\bar{b}X + c.c$	SM	no	5.84	0	0
	2		6.17	0.136	43.04
	SM	0.7 TeV $\leq m_{tb} \leq$ 1.1 TeV	0.14	0	0
	2		0.20	0.163	51.47
$pp \to W^+ZX + c.c$	SM	no	14.77	0	0
	3		16.96	0.570	180.37
	SM	0.7 TeV $\leq m_{WZ} \leq$ 1.1 TeV	0.20	0	0
	3		0.29	0.188	59.30
$pp \to W^+W^-X$	SM	no	29.86	0	0
	3		31.86	0.366	115.74
	SM	0.7 TeV $\leq m_{WW} \leq$ 1.1 TeV	0.37	0	0
	3		0.42	0.097	30.75

Table 3: Cross sections and statistical significance R of the model signals with respect to the SM for the studied processes when the integrated luminosity $\mathcal{L} = 100$ fb^{-1}. $R_0 = (\sigma_P - \sigma_{SM})/\sqrt{\sigma_{SM}}$.

lighter SM fermions.

The processes in which ρ interacts only to quarks of the third generation should be more sensitive to new physics than those which run through ρ-to-light-fermion vertices. However, at the LHC the former processes are often overwhelmed by a huge gluon-gluon background. We have seen this in the case of $pp \to t\bar{t}X$ and $pp \to b\bar{b}X$. We have demonstrated that also the processes where ρ couples to the light quarks in protons have a significant potential to distinguish our model from the light Higgs SM. We have calculated the statistical significance of the model signal for various decay channels of the final states. However, to decide whether and which of these channels can recognize the model at the LHC the further analysis, which would include the study of backgrounds and the detector reconstruction efficiency, is necessary. This is out of the scope of this paper, though. The results in this paper should help decide which of the processes are the best candidates for such further analyses.

References

[1] Cheng H-C, the proceedings of *15th International Conference on Supersymmetry and the Unification of Fundamental Interactions (SUSY07), Karlsruhe, Germany, 26 Jul - 1 Aug 2007*, hep-ph/0710.3407.

[2] Bando M, Kugo T, Yamawaki K, *Phys. Rep.* **164** (1988), 217.

[3] Coleman S R, Wess J, Zumino B, *Phys. Rev.* **177** (1969), 2239.

[4] Callan C G, Coleman S R, Wess J, Zumino B, *Phys. Rev.* **177** (1969), 2247.

[5] Casalbuoni R, et al., *Phys. Lett.* **B253** (1991), 275.

[6] Gintner M, Melo I, Trpišová B, the proceedings of *16th Conference of Czech and Slovak Physicists, Hradec Králové, Czech Republic, Sep 8 - 11, 2008*, in print.

[7] Gintner M, Melo I, Trpišová B, *Acta Phys. Slov.* **56** (2006), 473-483.

[8] Pukhov A, et al., hep-ph/9908288.

[9] Boos E, et al. (CompHEP Collaboration), *Nucl. Instrum. Meth.* **A534** (2004), 250.

final state	reduction factor r	P	cut	events (100 fb^{-1})	R (100 fb^{-1})
$pp \to t\bar{b}X + c.c.$					
$\ell^+\nu_\ell b\bar{b} + c.c$	$\epsilon_b^2 b_{\ell\ell}^W$	2	no	1.70×10^4	7.14
	0.0275		yes	5.40×10^2	8.53
$jjb\bar{b} + c.c$	$\epsilon_b^2 b_{jj}^W$	2	no	9.86×10^4	17.22
	0.16		yes	3.14×10^3	20.59
$pp \to W^+ZX + c.c.$					
$\ell^+\nu_\ell \ell'^+\ell'^- + c.c$	$b_{\ell\ell}^W b_{\ell\ell}^Z$	3	no	6.34×10^3	11.03
	0.0037		yes	1.08×10^2	3.63
$jj\ell^+\ell^- + c.c$	$b_{jj}^W b_{\ell\ell}^Z$	3	no	3.69×10^4	26.61
	0.0218		yes	6.26×10^2	8.75
$\ell^+\nu_\ell jj + c.c$	$b_{\ell\nu}^W b_{jj}^Z$	3	no	1.00×10^5	43.89
	0.0592		yes	1.70×10^3	14.43
$jjjj + c.c.$	$b_{jj}^W b_{jj}^Z$	3	no	5.84×10^5	105.84
	0.3443		yes	9.91×10^3	34.80
$jjb\bar{b} + c.c.$	$b_{jj}^W b_{bb}^Z \epsilon_b^2$	3	no	4.12×10^4	28.13
	0.0243		yes	7.00×10^2	9.25
$\ell^+\nu_\ell b\bar{b} + c.c.$	$b_{\ell\ell}^W b_{bb}^Z \epsilon_b^2$	3	no	7.12×10^3	11.69
	0.0042		yes	1.21×10^2	3.84
$pp \to W^+W^-X$					
$\ell_1^+\nu_{\ell_1}\ell_2^-\nu_{\ell_2}$	$(b_{\ell\ell}^W)^2$	3	no	3.86×10^4	12.73
	0.0121		yes	5.14×10^2	3.38
$\ell^+\nu_\ell jj$	$b_{\ell\ell}^W b_{jj}^W$	3	no	2.24×10^5	30.71
	0.0704		yes	2.99×10^3	8.16
$jjjj$	$(b_{jj}^W)^2$	3	no	1.30×10^6	74.07
	0.4096		yes	1.74×10^4	19.68

Table 4: Cross sections and statistical significance of the model signals for various decay channels of the analyzed processes. The integrated luminosity is $\mathcal{L} = 100\ \mathrm{fb}^{-1}$. The reduction factor r is the ratio between the cross sections of the process with the final state decayed and undecayed. The cut considered in Table is 0.7 TeV $\leq m_{34} \leq$ 1.1 TeV.